

LOW LOSS ACTIVE RADIAL MAGNETIC BEARING

Z Piech (*), M Hippner (**), S R Colby (*)

* United Technologies Research Center, 411 Silver Lane, East Hartford, CT 06108, USA

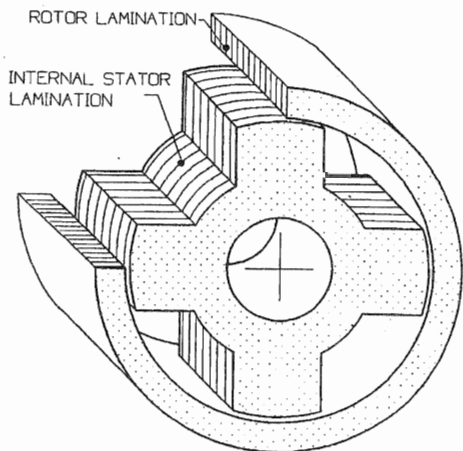
** Department of Electrical Engineering, University of Natal, Durban, Private Bag X10, Dalbridge 4014, South Africa

Abstract: A new type of biased radial magnetic bearing is described. The main advantage of the new type of bearing is a significantly reduced, as compared with other known magnetic bearings of this class, rotor core loss. The rotor core loss reduction is achieved by replacing a typical, salient pole stator, with the control winding concentrated on the stator poles, by a much more magnetically symmetrical structure, with the control winding placed in slots evenly distributed along the stator circumference. This leads to a much more even magnetic field distribution in the air gap between the stator and rotor, and consequently reduced rotor core loss. In the paper a method of rotor core loss calculation, based on a finite element magnetic field analysis, is described. The results of rotor core loss calculations for the two types of magnetic bearings, mentioned above, are also presented.

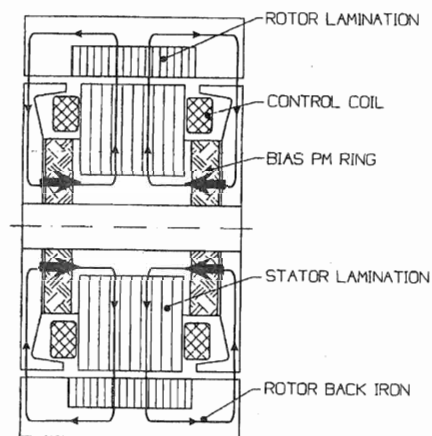
INTRODUCTION

A magnetic bearing system can be advantageous for rotating machinery due to the absence of mechanical wear, elimination of lubricating oil, and ability to operate at higher speeds than mechanical bearings. The forces required to support the rotating shaft are developed by an electromagnetic actuator, typically a part of a feedback control system. The electromagnetic actuator of a magnetic bearing has a rotating member (or rotor) and a stationary member (or stator) concentrically located with respect to each other. The rotor may be located concentrically internal or external to the stator. A magnetic bearing uses adjustable electromagnetic force generated by a current flowing

(a)



(b)



(c)

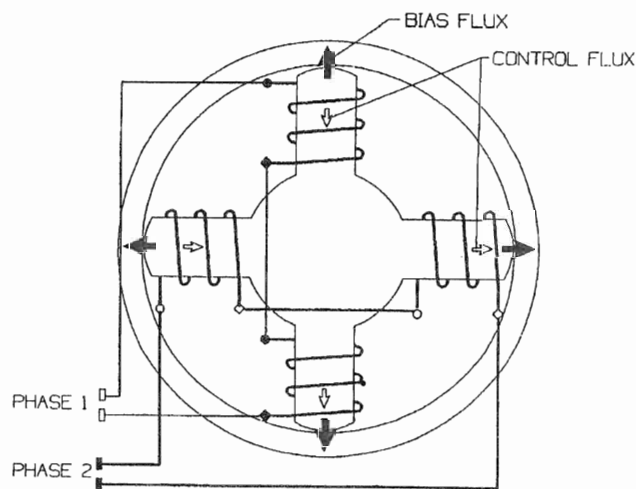


Fig. 1. Existing type of active radial magnetic bearing with external rotor: (a) rotor and stator laminations, (b) longitudinal section, (c) control winding

through coils wrapped around the stator poles and controlled by a control circuit, to adjust the distance between the stator and rotor. Also, proximity sensors are typically used to measure the length of the gap and to provide input signals to the control circuit. In addition to the variable electromagnetic control flux, a magnetic bearing may also have a constant DC bias flux, which premagnetizes the working air gaps to a specified level of the magnetic flux density. The bias linearises the control laws of the bearing. In some configurations, with a homopolar bias, a permanent

magnet can be used to provide the bias flux, eliminating the ohmic losses associated with the bias coils. Magnetic drag and iron losses are created whenever the rotor rotates within a spatially varying bias magnetic flux. Certain high-speed applications such as flywheel energy storage systems are very sensitive to rotor heating caused by core losses in the bearing rotor, and to the magnetic drag caused by losses in the rotor iron. The higher the speed the greater the losses, and increased heat can demagnetise permanent magnets which may be embedded in the rotor. Furthermore, if the rotor is located in a vacuum containment vessel, as in the case of energy storage flywheel devices, it may be difficult to cool the spinning mass. A magnetic bearing design with very low rotor loss would be advantageous for such critical applications.

Novel homopolar magnetic bearing concepts were described and patented by Malsky [1] and Meeks [2]. These concepts employ a homopolar flux to bias the stator poles to the same polarity, e.g. all are 'north' poles. Control windings direct the flux at opposite poles to one side of the stator or the other to produce a control force in the axis of the poles. Fig. 1 shows the configuration of the homopolar bearing with four poles, described in the patent [1]. The rotor lamination is subjected to a time varying magnetic flux as it rotates through the spatially varying time-invariant bias flux. The perceived advantage of the homopolar bearing is that the bias flux is of one polarity, hence the variation in the rotor flux will be reduced, and the rotor losses should be reduced relative to a bipolar magnetic bearing. Despite this feature, the resulting eddy current and hysteresis rotor losses, caused by discontinuities or sharp changes in the flux distribution along the air gap circumference (Fig. 4 (a) and (b)) can be unacceptable in certain applications, where an extremely low magnetic drag is required or where rotor heating is critical.

PROPOSED MAGNETIC BEARING

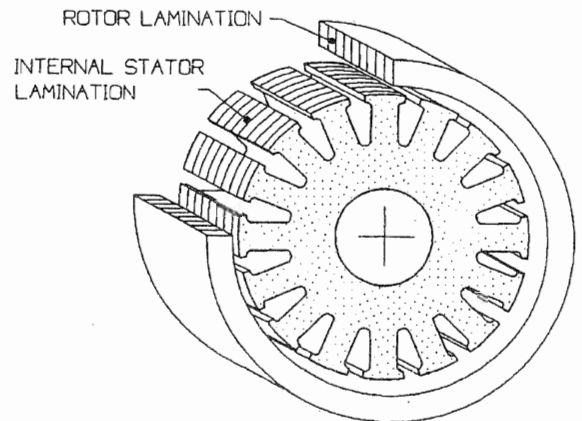
The proposed system addresses the application of a new radial homopolar magnetic bearing with a significant reduction of the rotor loss, as compared with the bearing described in patent [1] or [2]. A new magnetic bearing is designed with a different configuration of the stator lamination stack, which results in a more even spatial distribution of the bias flux in the air gap. In conjunction with the new shape of stator lamination, a different configuration of the control windings is employed to take advantage of the uniform distribution of the bias flux.

Magnetic Configuration

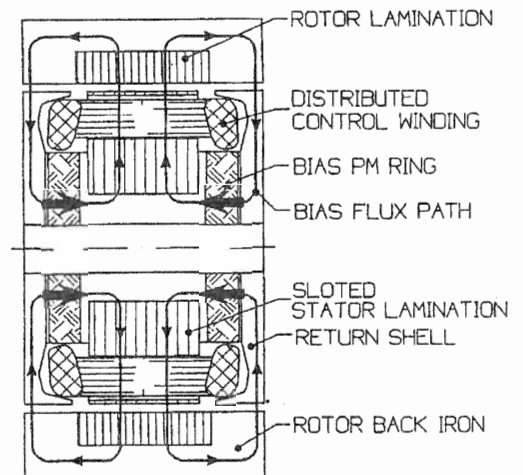
A layout of the new bearing is shown in Fig. 2 (a). The depicted configuration is that of an external rotor bearing, but this could be turned 'inside out' to yield an internal rotor bearing. The longitudinal section in Fig. 2 (b) shows the arrangement of the stator and rotor lamination stacks, permanent magnets creating the bias flux, and the bias flux

path. The permanent magnets are oriented in axial opposition at either end of the stator lamination stack. The resulting flux travels radially outward through the stator stack, across the air gap, and radially through the rotor lamination stack to the rotor back iron. The bias flux then returns axially through the back iron and across the air gap to the bias flux return shells, closing its path to the

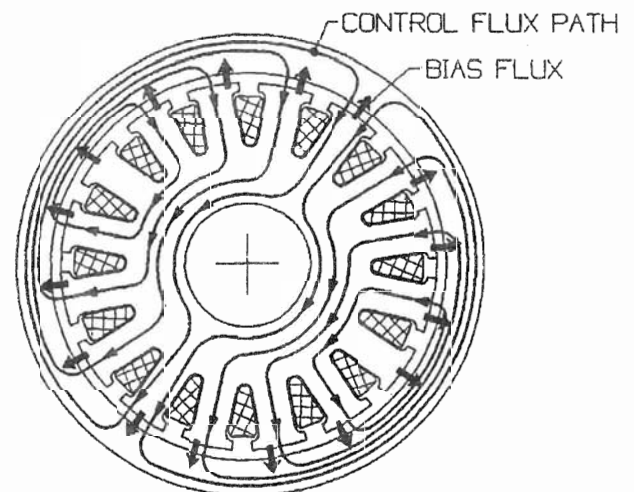
(a)



(b)



(c)



(d)

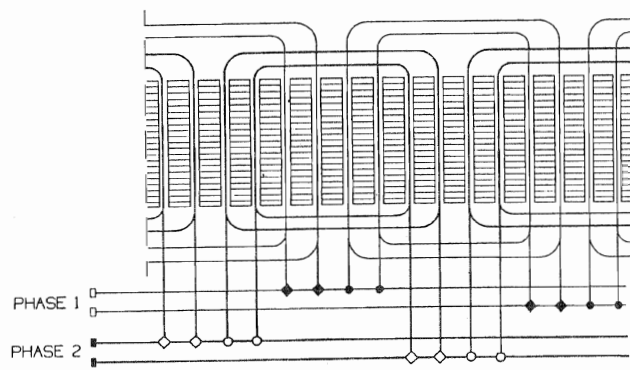


Fig. 2. A new type of active radial magnetic bearing: (a) rotor and stator lay out, (b) cross-section, (c) longitudinal section, (d) control winding

permanent magnet rings. There are other possible orientations of the bias permanent magnets but they are not discussed here. The cross-section in Fig. 2 (c) shows the stator lamination, with slots for a polyphase, two-pole, sinusoidally distributed winding. The bias flux produced by permanent magnets, is directed radially outward over the entire surface of the stator stack. The bias flux is spatially uniform, except for a minor perturbation due to the stator slot openings. The bias flux in the rotor is invariant with angular position, hence there is no time variation of the bias flux in the rotor and no rotor core loss. The arrangement of control coils must be a two-pole, sinusoidally distributed, polyphase winding. Any number of phases is possible, although two phase and three phase are the most practical configurations. A two phase winding is shown in Fig 2 (d). The currents flow through the control winding generating the control flux flow in the bearing lamination. The control magnetic flux is distributed in a similar way as it is in a polyphase electric machine. In one half of the air gap circumference, the control flux flows in the same direction as the bias flux, increasing the magnetic flux density in that portion of the air gap. In the second half of the air gap circumference, the control flux is directed in the opposite direction to the bias flux, reducing the resultant magnetic flux density completely or partially, depending on the value of the control current.

Principle of Operation

The bias flux density $B_b(\theta)$ is distributed uniformly around the air gap of the stator lamination stack and is expressed as:

$$B_b(\theta) = B_o \quad (1)$$

Polyphase currents in the control windings produce a 2-pole distribution of the control flux density $B_c(\theta)$ around the gap:

$$B_c(\theta) = B_1 \cdot \cos(\theta + \alpha) \quad (2)$$

where:

B_1 = the maximum value of the control flux density,

θ = variable angle,

α = angle of circumferential location of the external force exerted on the rotor.

The net radial air gap flux density is the vector sum of the two components:

$$B_g(\theta) = B_o + B_1 \cdot \cos(\theta + \alpha) \quad (3)$$

The force acting on the rotor in the α direction, which is taken as an angle from the magnetic axis of the stator winding, is:

$$F_\alpha = \frac{L \cdot R}{2 \cdot \mu_o} \cdot \int B_g^2(\theta) \cdot \cos(\theta + \alpha) \cdot d\theta \quad (4)$$

L = stack length (in axial direction),

R = rotor internal radius.

Substituting eq. (3) into eq. (4) yields:

$$F_\alpha = \frac{L \cdot R}{2 \cdot \mu_o} \cdot \pi \cdot B_o \cdot B_1, \quad (5)$$

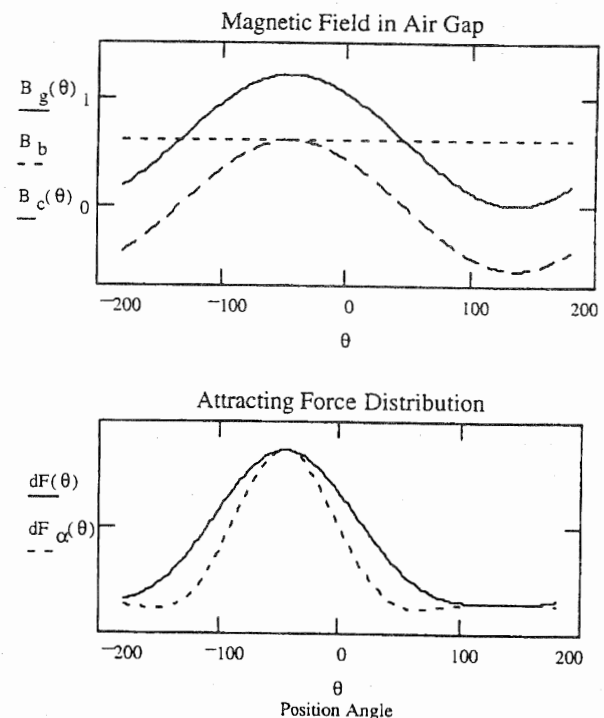


Fig. 3. Distribution of magnetic flux density and force density around the rotor surface, for the control current giving the maximum force at $\alpha = -45^\circ$ from the magnetic axis of the winding

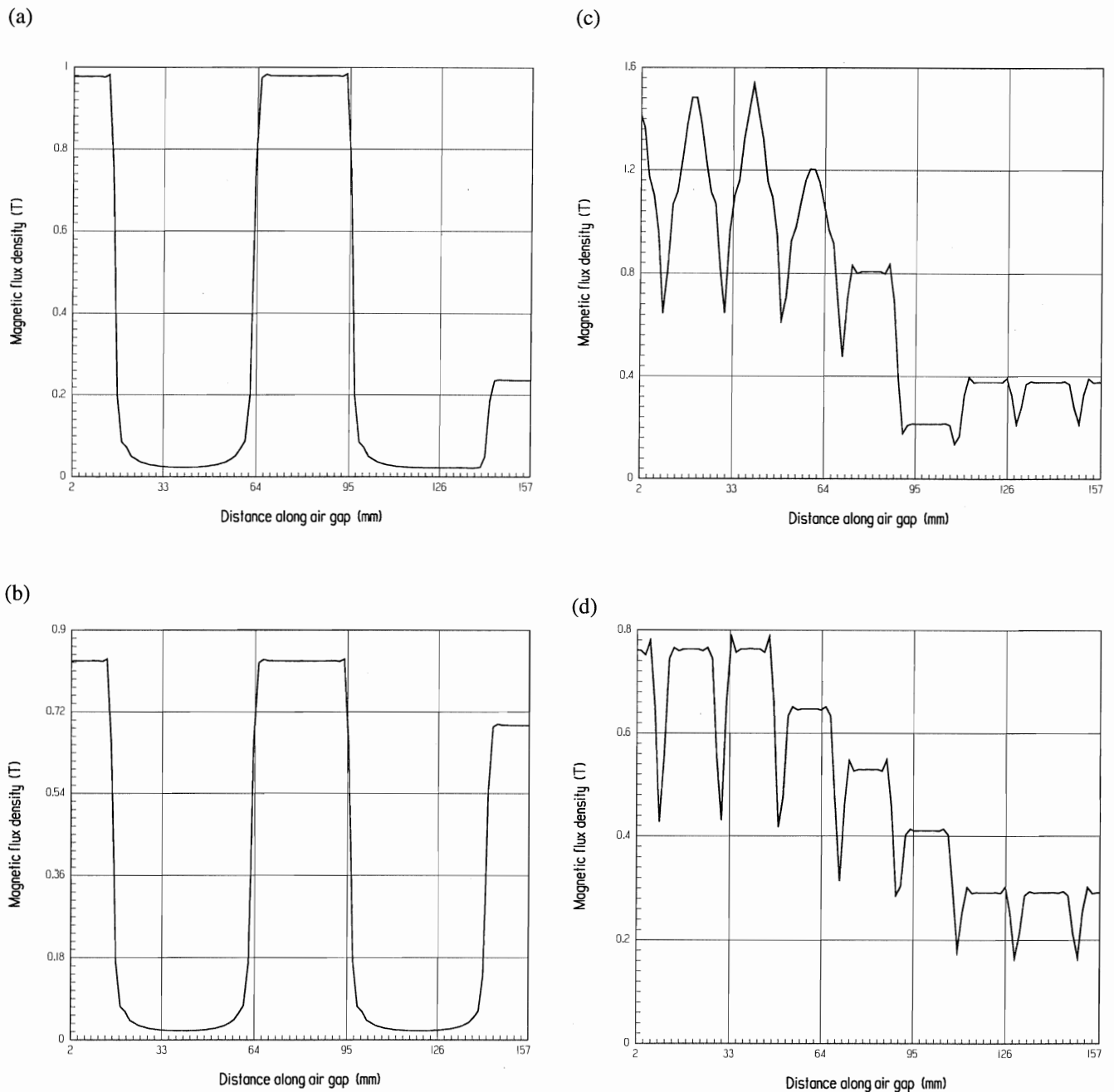


Fig. 4. Magnetic flux distribution along the air gap between the stator and rotor (half of the circumference plotted): (a) existing type bearing at full control current, (b) existing type bearing at 20 % of control current, (c) new type bearing at full control current, (d) new type bearing at 20 % of control current.

FINITE ELEMENT ANALYSIS

A finite element analysis of both the existing and new type of magnetic bearing was performed. The main objective of this analysis was to calculate the magnetic field distribution in the rotor. The results of this analysis were in turn used to calculate the rotor iron loss, as described in the next section. The finite element analysis also provided interesting results which explain a lower rotor iron loss in the new type bearing. Fig. 4 (a) and (b) show the magnetic flux density

distribution in the air gap of the existing type bearing, for two different values of the control current. It is clearly visible that the magnetic flux density changes rapidly from its maximum value, at the stator pole area, to practically zero, at the stator interloper area. The magnetic flux density distribution in the air gap of the new type bearing is shown in Fig. 4 (c) and (d). One can notice a much less violent, almost sinusoidal distribution, with dips due to the stator slots only. One should also notice four periods of the magnetic flux density change (four maxima and four

minima) when travelling along the stator of the existing bearing, while only one such period can be observed in the case of the new type bearing. This means that at the same rotational speed the rotor of the proposed bearing would be subjected to a four times lower frequency of magnetic field than the rotor of the existing bearing. All these contributes towards a much lower rotor loss of a new type bearing.

ROTOR IRON LOSSES EVALUATION

The iron loss evaluation is performed only for the rotor lamination. The solid rotor backiron (outside the lamination) conducts the uniformly distributed constant bias flux. Moreover, if any changes in the magnetic field distribution on the surface of rotor solid ring occur, the skin effect reduces the affected area to negligible depth, (for example, the magnetic field equivalent penetration depth for 4340 Steel at frequency 583 Hz - 35,000 RPM is about 0.7 mm). In conclusion, it can be assumed that the solid backiron of the rotor does not produce significant power losses due to magnetic field variation.

For loss analysis the rotor lamination is divided into five layers (five concentric rings in radial direction). The finite element analysis provides distribution of the magnetic field in each layer of the rotor. The field distribution in each layer is different and depends on the level and direction of the external load. The radial and tangential component of the magnetic field density are separately analysed using the Fast Fourier Transform. The spectrum of harmonics is used to calculate the hysteresis and eddy current losses. The harmonics magnitudes of field spectrum lower than 0.025 T are neglected to simplify the calculation.

The unit hysteresis loss for sinusoidal signal with magnitude B_{mk} and frequency f_k can be computed as follows:

$$\Delta P_{hlk}^{(r)} \approx \frac{f_{fk}}{f_u} \cdot \left(\frac{B_{mk}^{(r)}}{B_u} \right)^K \cdot \frac{k_{he}}{1 + k_{he}} \cdot \Delta P_u, \quad (6)$$

where:

l = layer number,

k = harmonic number,

ΔP_u = unit power loss for frequency $f_u = 50$ Hz and $B_u = 1$ T (for Rotelloy5 used in calculation ; $\Delta P_u = 3.75$ W/kg),

K = power factor for hysteresis loss, varies between 1.5 and 2.5 depending on the magnetic flux density,

(r) = indicates the radial component,

k_{hu} = ratio of hysteresis unit loss to eddy current unit loss (Rotelloy5, 0.014"; $k_{hu} = 6.2$ [3]).

The unit eddy current loss can be computed by a similar formula:

$$\Delta P_{elk}^{(r)} \approx \left(\frac{f_{fk}}{f_u} \right)^\beta \cdot \left(\frac{B_{mk}^{(r)}}{B_u} \right)^2 \cdot \frac{1}{1 + k_{he}} \cdot \Delta P_u, \quad (7)$$

β = power factor for eddy current loss, varies between 1.5 and 2.0 depending on material.

Formula (6) and (7) are also used to calculate loss due to the tangential component of the magnetic flux density (t).

After computing the unit power loss, separately for the radial and tangential components of the magnetic flux density B , for each harmonic, the total hysteresis and eddy current loss for each rotor layer can be found by multiplying the unit loss by the mass of each layer.

$$P_{hl}^{(r)} = G_l \cdot \sum_{k=1}^N \Delta P_{hlk}^{(r)} \quad (8)$$

$$P_{el}^{(r)} = G_l \cdot \sum_{k=1}^N \Delta P_{elk}^{(r)} \quad (9)$$

Finally, the bearing total hysteresis and eddy current loss as for the radial (r) component are described as follows:

$$P_h^{(r)} = \sum_{l=1}^5 P_{hl}^{(r)} \quad (10)$$

$$P_{el}^{(r)} = \sum_{l=1}^5 P_{el}^{(r)} \quad (11)$$

Similar operations are done for the tangential component (t).

Total bearing iron loss produced due to the variation of both radial and tangential components of the magnetic field can not be computed simply by adding losses obtained separately for both components by formulas (10) and (11). It could be allowed only for eddy current losses when magnitudes for both components are the same (pure rotational magnetization) [5], [6]. In the other case when $B_{mk}^{(t)} \geq B_{mk}^{(r)}$, (for elliptical magnetization), the eddy current losses can be computed by the formula:

$$P_{ek} = P_{ek}^{(t)} \cdot \left[1 + \left(\frac{B_{mk}^{(r)}}{B_{mk}^{(t)}} \right)^2 \right] \quad (12)$$

A more complicated calculation process must be applied for computing of the hysteresis losses. The proportion between losses produced with rotational magnetization ($B_{mk}^{(t)} = B_{mk}^{(r)}$) and losses produced with axial magnetization ($B_{mk}^{(t)} = 0$ or $B_{mk}^{(r)} = 0$) depend on the magnetic flux density. The relation between the hysteresis losses at rotational magnetization and losses at axial magnetization was analysed and published for the first time by Brailsford,

[4]. However, in the homopolar bearings considered in this paper, each part of the rotor lamination is magnetized with elliptical field. Therefore, application of the relationship between $B^{(t)}$ and $B^{(r)}$ proposed by Brailsford, ref. [4] is not valid.

Measurements and a 'cut and try' method indicate that use of the geometrical sum of the losses due to the tangential and radial components of the magnetic flux density gives good results for approximation of the total hysteresis losses for magnetic bearings:

$$F_h = \sqrt{(P_h^{(t)})^2 + (P_h^{(r)})^2} \quad (13)$$

The total bearing losses are obtained by summation of eddy current and hysteresis losses:

$$P = P_h + P_e \quad (14)$$

The computed power loss for the existing homopolar bearing [1] and proposed magnetic bearing are compared in Table 1. Both bearings were designed for the load of 270 N, with the inner diameter of the external rotor 102 mm, the lamination stack length of 19 mm and the stack thickness of 10 mm.

Table 1. Comparison of rotor losses at 20% of load (control current 2 A), and at full load (control current 10 A).

Bearing Type	Rotor Losses (W)			
	Rotor Speed 17,000 RPM		Rotor Speed 35,000 RPM	
	20% Load	100% Load	20% Load	100% Load
<i>Existing</i>	25.3	36.1	64.5	92.9
<i>New</i>	1.6	23.0	4.7	58.4

CONCLUSIONS

A new type of a homopolar radial magnetic bearing was introduced. The proposed bearing, due to a specific stator structure and control winding design, has significantly reduced rotor iron loss, as compared with other known magnetic bearings of that class.

The rotor iron loss computations showed that the rotor iron loss of the proposed bearing, was respectively 6% and 64%, depending of the bearing load, of the loss computed for the existing [1] bearing. A lower value (6%) was computed for 20% of full load. The above results, obtained using an approximate theoretical model of iron losses, require an experimental validation.

References

1. Malsky, "High-Speed, Low-Loss Antifriction Bearing Assembly", US Patent No. 5,179,308; 1993.
2. Meeks C R, "Magnetic Bearing Structure", US Patent No. 5,111,102; 1992.
3. Dabrowski M: "Magnetic Circuit Core Power Losses", Warsaw - Poznan, PWN 1981, Poland.
4. Brailsford: "Rotational Hysteresis Loss in Electrical Sheet Steels", Institution of Electrical Engineers Journal, 1928, p.566.
5. Zhu J G, Ramsden V S, Watterson P A: "Finite Element Calculation of Core Losses in Motors with Non-Sinusoidal Fields", International Conference on Electrical Machines, Manchester, 1992, pp. 1182-1186
6. Zhu J G, Ramsden V S: "Core Loss Modelling in Rotational Electrical Machines", International Conference on Electrical Machines in Australia, Adelaide, 1993, pp. 52-57